Chapter 2. Basic Atomic Physics

Academic and Research Staff

Professor Daniel Kleppner, Professor David E. Pritchard, Professor Wolfgang Ketterle

Visiting Scientists and Research Affiliates

Dr. Theodore W. Ducas,[1] Dr. Alan L. Lenef, Dr. Fred L. Palmer, Dr. H. Jörg Schmiedmayer

Graduate Students

Michael R. Andrews, Michael P. Bradley, Michael S. Chapman, Michael W. Courtney, Kendall B. Davis, Frank DiFilippo, Joel C. DeVries, Troy D. Hammond, Jeffrey R. Holley, Hong Jiao, Robert I. Lutwak, Marc-O. Mewes, Richard A. Rubenstein, Edward T. Smith, Neal W. Spellmeyer

Undergraduate Students

Ilya Entin, Philip M. Hinz, Wan Y. Morshidi, Amrit R. Pant, Szymon M. Rusinkiewicz, Abraham D. Stroock, Bridget E. Tannian, Stanley H. Thompson, John J. Wuu, Peter S. Yesley

Technical and Support Staff

Carol A. Costa

2.1 Studies in Quantum Chaos: High Resolution Periodic Orbit Spectroscopy

Sponsors

Joint Services Electronics Program
Contract DAAL03-92-C-0001
Grant DAAH04-95-1-0038
National Science Foundation
Grant PHY 92-21489
U.S. Navy - Office of Naval Research
Grant N00014-90-J-1322

Project Staff

Michael W. Courtney, Hong Jiao, Neal W. Spellmeyer, Professor Daniel Kleppner

Our understanding of Rydberg atoms in strong fields has been advanced by high resolution spectroscopy, the development of efficient quantum calculations for atoms in electric and magnetic fields, and theoretical advances in classical dynamics. The principal motivation for this work is to understand atomic systems under external perturbations that are comparable to the unperturbed energy and in which the classical motion may be irregular. Rydberg atoms are central to this research because their atomic fields are comparable to the field strengths available in the laboratory. In addition, with the important exception of the hydrogen atom in an electric field, the classical counterparts of these systems all undergo a transition from order to chaos. Consequently, Rydberg atoms in applied fields provide a natural testing ground for studying the connections between quantum mechanics and classical chaos.

In the semiclassical limit, periodic orbit theory provides a unifying principle for relating a quantum spectrum to the periodic orbits of the corresponding classical system. According to periodic orbit theory, each periodic orbit produces a sinusoidal modulation in the density of states. Quantum mechanically, a spherical wave sent out from the origin will recur (overlap with the original outgoing wave) at times corresponding to the periods of the periodic orbits of the classical system. The magnitude of this overlap gives the strength of the modulation of the spectrum.

In our laboratory, we have studied lithium in an electric field, a system that displays a transition from order to core-induced chaos. In contrast, the classical dynamics of hydrogen in an electric field is always orderly. Its Hamiltonian

$$H = \frac{1}{2}p^2 - \frac{1}{r} + Fz$$

[1] Physics Department, Wellesley College, Wellesley, Massachusetts.

can be rescaled using the substitutions $r = F^{-1/2}\tilde{r}$ and $p = F^{1/4}\tilde{p}$. Because the scaled Hamiltonian

$$\tilde{H} = \frac{1}{2}\tilde{p}^2 - \frac{\tilde{1}}{r} + \tilde{z}$$

does not depend explicitly on the field, the classical dynamics depends only on the scaled energy $\varepsilon = EF^{-1/2}$, not on E and F separately. This classical scaling is exact for hydrogen and a good approximation for lithium.

The scaled action of a particular closed orbit, $\tilde{S}_k = F^{-1/4}S_k$, depends only on ε. If the spectrum is recorded while the field and the energy are varied simultaneously to keep ε constant, the classical dynamics remains the same. This approach has been applied to several systems,[2] but we have extended it to a higher resolution than previously possible.

An orbit's scaled action and recurrence strength can be obtained directly from the Fourier transform of the spectrum. This Fourier transform is called the *recurrence spectrum* because each peak is located at the scaled action of a periodic orbit. The height of a peak is proportional to that orbit's recurrence strength. We have applied this approach to the lithium Stark spectrum. To model the atomic core potential of lithium, we have added to the hydrogenic Hamiltonian a short range potential, chosen to give the proper quantum defects. Within these constraints a variety of model potentials yields essentially the same classical behavior. In particular, as the scaled energy is increased, lithium shows a transition from regular to chaotic motion at about $\varepsilon = -16$.

We have carried out laser spectroscopy on an atomic beam of lithium in an applied electric field. The atomic beam passes through holes in the centers of a pair of electric field plates. Between the field plates, one laser (735 nm) excites the 2S → 3S two-photon transition, and a second laser (610 nm), polarized parallel to the external field, excites Rydberg states. These states are field ionized and ions are detected by a channeltron. The error in scanning the laser to maintain constant scaled energy is 0.002 cm^{-1}; the fractional error in the electric field is 0.3 percent.

To verify our methods, the experimental recurrence spectrum at $\varepsilon = -3.0$ is compared with a recurrence spectrum obtained from quantum computations in figure 1.[3] Agreement is generally good, although there are some small discrepancies that we believe arise from experimental noise and neglect of the continuum in the computations. Closed orbits parallel to the field play an important role in the spectrum. These form two classes: "uphill" orbits, directed toward the cathode, and the "downhill" orbits, directed toward the anode. For $\varepsilon = -3.0$, the first return of the uphill orbit has a scaled action of 0.3915, and the first return of the downhill orbit has a scaled action of 0.4285. As a result, the recurrence spectrum should have peaks at 0.3915 n and 0.4285 n. In figure 2, most of the prominent peaks for scaled action less than 10 are identified as corresponding to repetitions of the parallel orbits. For high action, the parallel orbits continue to display a strong signature in the spectrum. We have identified recurrences near the 100th return of the uphill parallel orbit (figure 3). This illustrates the power of closed-orbit theory to associate spectral features with long-period orbits.[4]

Gao and Delos[5] recently examined closed orbits and recurrences for single electron atoms in electric fields. At high energy (positive energy regime), only one closed orbit, parallel to the field and extending from the nucleus to the classical turning point, exists. The spectrum contains a fundamental Fourier component from this orbit plus harmonics and its repetitions. As the energy is decreased, new orbits are predicted to spring into existence by an orderly sequence of bifurcations. At each bifurcation, a new frequency component is added to the spectrum. To study these bifurcation processes near the ionization limit of lithium in an electric field, we have performed scaled-energy spectroscopy on m=0 states of lithium for scaled energy between $\varepsilon =$

---

2 A. Holle, J. Main, G. Wiebusch, H. Rottke, and K.H. Welge, *Phys. Rev. Lett.* 61(13): 161 (1988); T. van der Veldt, W. Vassen, and W. Hogervorst, *Europhys. Lett.* 21: 9 (1993); U. Eichmann, K. Richter, D. Wintgen, and W. Sander, *Phys. Rev. Lett.* 61: 2438 (1988).

3 M.L. Zimmermann, M.G. Littman, M.M. Kash, and D. Kleppner, "Stark Structure of the Rydberg States of Alkalimetal Atoms," *Phys. Rev. A* 20: 2251 (1979).

4 M. Courtney, H. Jiao, N. Spellmeyer, and D. Kleppner, "Long-Period Orbits in the Stark Spectrum of Lithium," *Phys. Rev. Lett.* 73: 1340 (1994).

5 J. Gao and J.B. Delos, "Resonances and Recurrences in the Absorption Spectrum of an Atom in an Electric Field," *Phys. Rev. A* 49: 869 (1994).

-2.1 and ε = -0.37. A map of the recurrence spectra is shown in figure 4. We observe small recurrences corresponding to repetitions of the parallel orbit, and large recurrences near bifurcations. The large bifurcation peaks are labeled with the fractions, m/l, used to designate the newly created orbits. These orbits are displayed in figure 4. Our experimental study reveals that the bifurcation of classical trajectories dominates the spectrum, and bifurcation theory provides a natural way of understanding the evolution of the spectrum from a broad continuum above the ionization limit to a quasi-discrete spectrum below the ionization limit.[6]

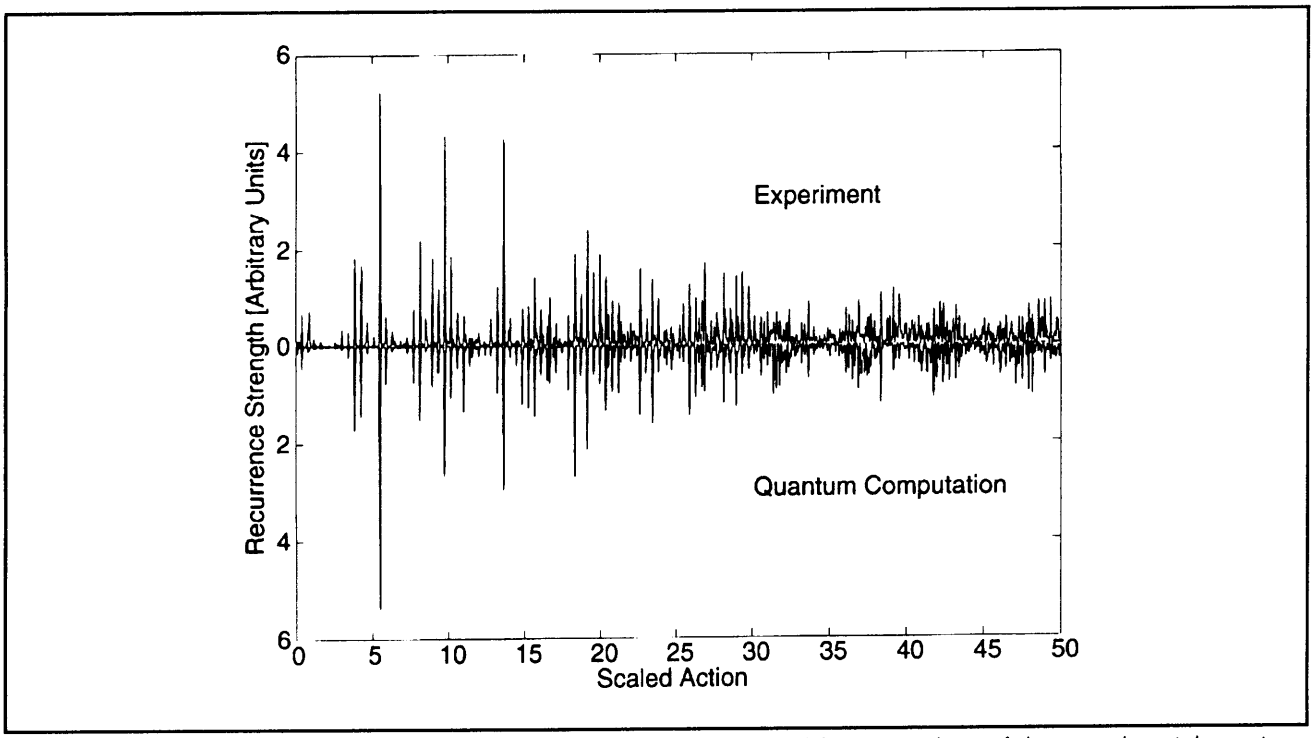

Figure 1. Lithium recurrence spectrum for ε = -3.0. A mirror plot is used for comparison of the experimental spectrum (top) with the results of a quantum computation (bottom). The computed spectrum has been normalized to provide comparable heights.

2.1.1 Publications

Courtney, M., H. Jiao, N. Spellmeyer, and D. Kleppner. "Quantum Chaos and Rydberg Atoms in Strong Fields." *Drexel Conference Proceedings.* Forthcoming.

Courtney, M., N. Spellmeyer, H. Jiao, and D. Kleppner. "Classical, Semiclassical, and Quantum Dynamics in the Lithium Stark System." *Phys. Rev. A.* Forthcoming.

Courtney, M., and D. Kleppner. "Core-Induced Chaos in Diamagnetic Lithium." *Phys. Rev. A.* Forthcoming.

Courtney, M., H. Jiao, N. Spellmeyer, D. Kleppner, J. Gao, and J.B. Delos. "Closed Orbit Bifurcations in Continuum Stark Spectra." *Phys. Rev. Lett.* 74: 1538 (1995).

Courtney, M., H. Jiao, N. Spellmeyer, and D. Kleppner. "Long-period Orbits in the Stark Spectrum of Lithium." *Phys. Rev. Lett.* 73: 1340 (1994).

2.1.2 Theses

Courtney, M. *Rydberg Atoms in Strong Fields: A Testing Ground for Quantum Chaos.* Ph.D. diss., Dept. of Physics, MIT, 1994.

[6] M. Courtney, H. Jiao, N. Spellmeyer, and D. Kleppner, "Closed Orbit Bifurcations in Continuum Stark Spectra," *Phys. Rev. Lett.* 74: 1538 (1995); M. Courtney, *Rydberg Atoms in Strong Fields: A Testing Ground for Quantum Chaos,* Ph.D. diss., Dept. of Phys., MIT, 1995.

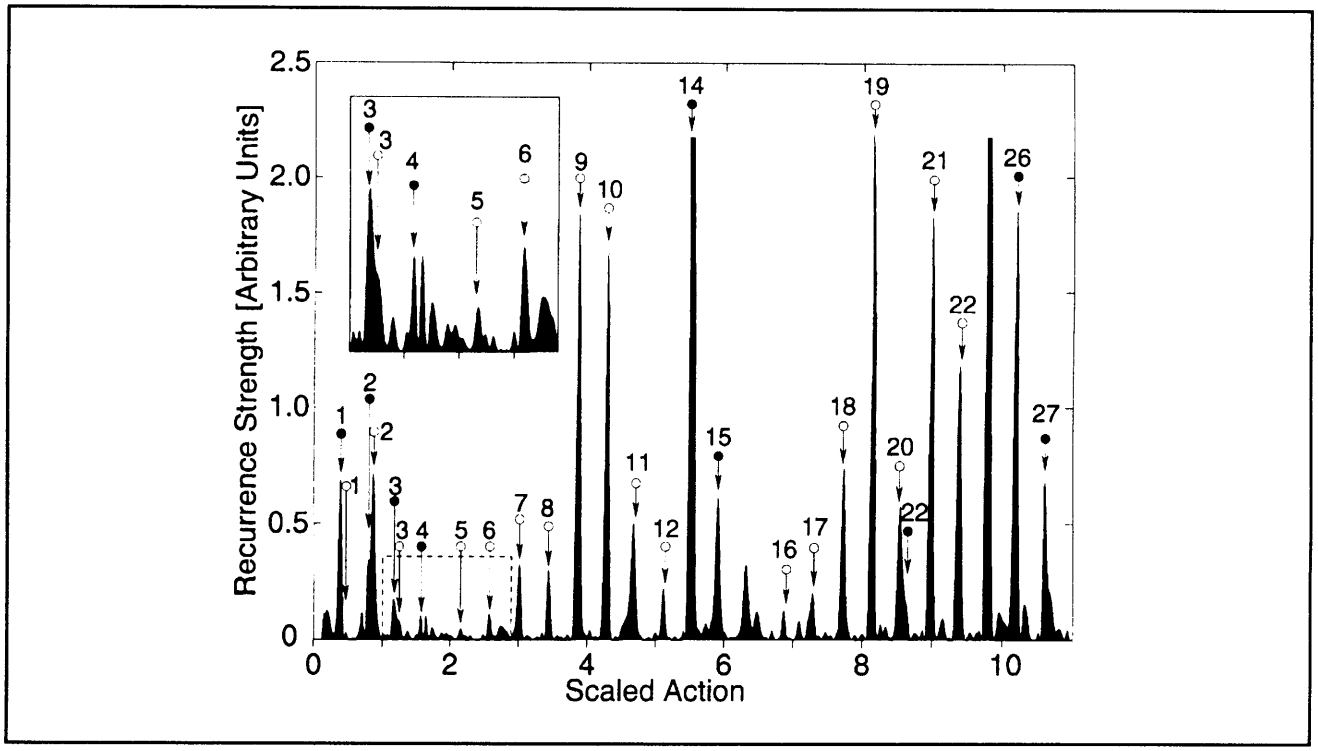

Figure 2. Blowup of experimental data in figure 1. Recurrences corresponding to the parallel orbits are marked with arrows. Filled circles: uphill orbits. Open circles: downhill orbits. The number specifies the number of repetitions of the primitive orbit. The truncated peak at scaled action of 5.5 has strength 5.2. The truncated peak at scaled action of 9.8 has strength 4.3. The inset shows detail near scaled action of 2.

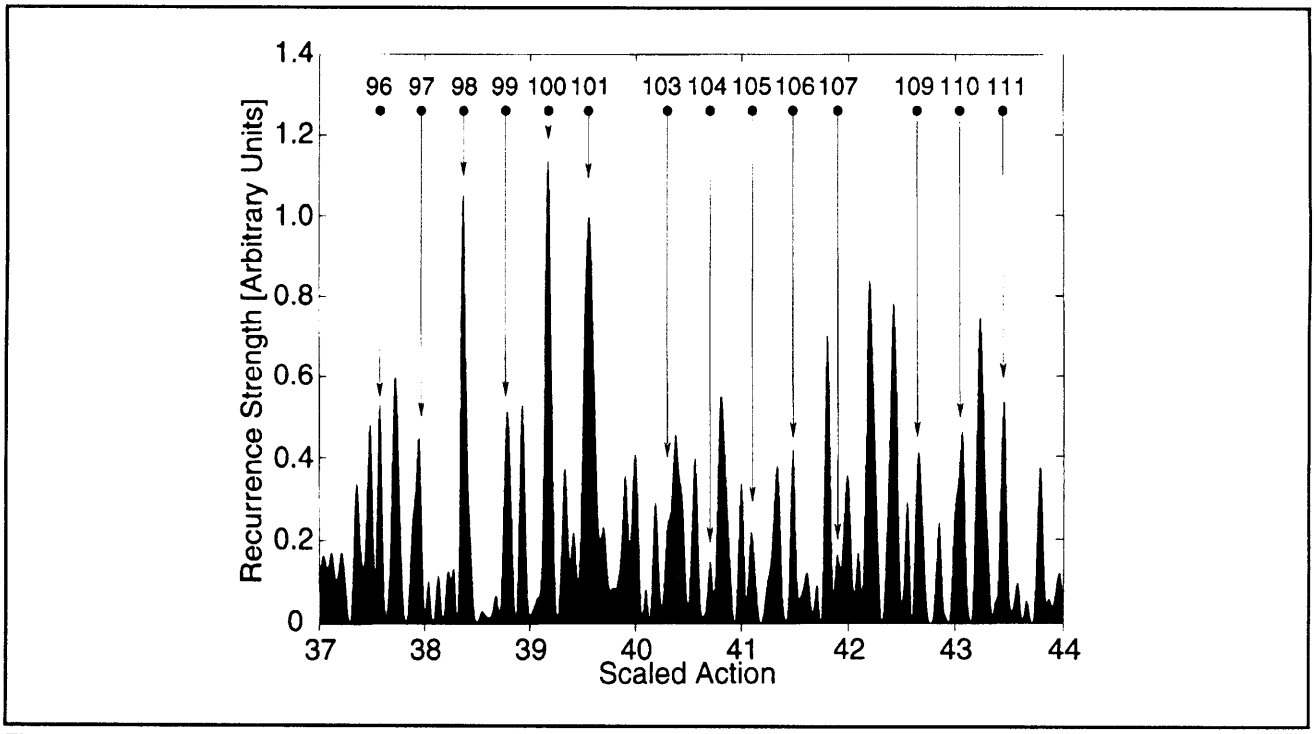

Figure 3. Blowup of figure 1 at large action. Peaks identified with uphill parallel orbits are marked with arrows, as in figure 2.

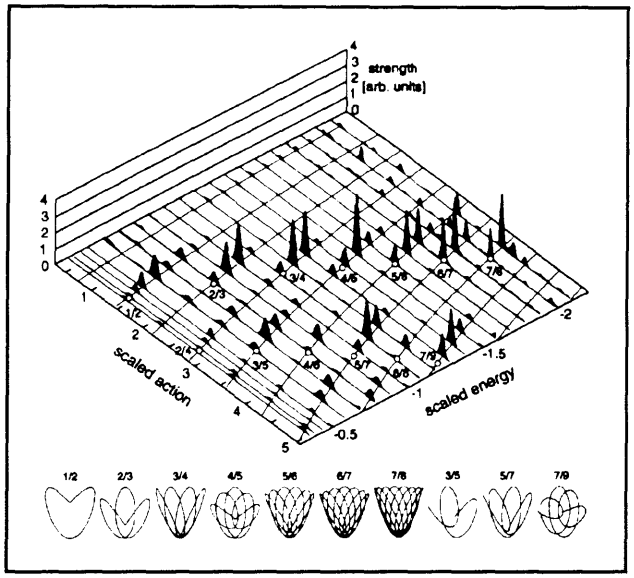

Figure 4. The curves in the horizontal plane represent the scaled action of the parallel orbit and its repetitions as a function of scaled energy. Locations of bifurcations are marked with small open circles. New orbits created in bifurcations have almost the same action as the corresponding return of the parallel orbit. Measured recurrence strengths are shown in the z direction. Recurrences are especially strong at scaled energies slightly lower than bifurcations. Orbits created by bifurcation of the parallel orbit are shown along the bottom. The 2/4, 4/6 and 6/8 orbits are repetitions of the 1/2, 2/3 and 3/4 orbits respectively, so their shapes are identical.

2.2 Determination of the Rydberg Frequency

Sponsor

Joint Services Electronics Program
Contract DAAL03-92-C-0001
Grant DAAH04-95-1-0038
National Science Foundation
Grant PHY 92-21489

Project Staff

Joel C. DeVries, Dr. Theodore W. Ducas, Jeffrey R. Holley, Robert I. Lutwak, Professor Daniel Kleppner

The Rydberg constant, R_∞, relates the atomic unit of distance to laboratory units. It is a so-called fundamental constant, and recent advances in laser optical spectroscopy have made it possible to measure it with accuracy approaching 2 parts in 10^{11}.[7] The Rydberg *frequency,* cR_∞, relates the atomic unit of frequency to laboratory units. Although the speed of light c is an exactly defined quantity, the relation between the Rydberg constant and the Rydberg frequency is not merely formal: the precision with which a frequency can be measured is limited in principle to the precision of atomic clocks, which currently exceeds 1 part in 10^{14} and is expected to grow even larger. In contrast, wavelength metrology appears to have reached its limit of precision, somewhat less than 1 part in 10^{11}.

To make full use of the precision of lasers and modern laser spectroscopy, and for applications in communications, control, and metrology, general techniques for measuring the frequency of light need to be developed. As part of this effort, we propose to help establish a new optical frequency standard by measuring the Rydberg frequency.

Our approach involves measuring the frequency of transitions in atomic hydrogen at wavelengths long enough for the frequency to be measured directly by an atomic clock. The experiment employs a highly excited "Rydberg" state of atomic hydrogen, n=29, and involves measuring transitions to nearby states at frequencies of approximately 256 GHz. This signal is generated coherently from a frequency standard based on an atomic clock.

The goals of our experiment are three-fold: First is the reevaluation of R_∞ itself, providing an independent check, in a different regime, of other evaluations based on optical wavelength metrology. Second is the measurement of the ground state Lamb shift. Because our measurements involve high angular momentum states for which the Lamb shift is extremely small, our results may be compared with optical measurements of transitions between low-lying states to yield an improved measurement of the Lamb shift. Third is to provide a frequency calibration of the spectrum of hydrogen, enabling the creation of a comprehensive frequency standard extending from the radio-frequency regime to the ultra-violet.

Our experiment employs an atomic beam configuration to reduce Doppler and collisional perturbations. Atomic hydrogen is excited to the low angular momentum n=29, m=0 state by two-photon stepwise absorption from a pulsed laser source. The excited atoms are then transferred to the longer lived n=29, m=28 "circular" state by absorption of

[7] T. Andreae et al., "Absolute Frequency Measurement of the Hydrogen 1S-2S Transition and a New Value of the Rydberg Constant," *Phys. Rev. Lett.* 69(13): 1923-1926 (1992); F. Nez et al., "Precise Frequency Measurement of the 2S-8S/8D Transitions in Atomic Hydrogen: New Determination of the Rydberg Constant," *Phys. Rev. Lett.* 69(16): 2326-2329 (1992).

circularly polarized radio-frequency radiation.[8] The atoms enter a region of uniform electric field in which the frequency of the transition (n=29, m=28) → (n=30,m=29) is measured by the method of separated oscillatory fields. The final state distribution is analyzed by electric field ionization. The resonance signal appears as a transfer of atoms from the n=29 state to the n=30 state as the millimeter-wave frequency is tuned across the transition.

Figure 5 illustrates the apparatus. Atomic hydrogen or deuterium is produced by dissociating H_2 or D_2 in a radio-frequency discharge. The beam is cooled by collisions in a cryogenic thermalizing channel in order to slow the beam and thereby increase the interaction time. The atoms enter the circular state production region, where they are excited from the 1s ground state, through the 2p state, to the n=29, m=0 state by two-photon stepwise excitation. The laser excitation is performed in an electric field to provide selective population of a particular n=29, m=0 level. The electric field is then rapidly reduced to an intermediate value as the atoms pass through the center of a circle of four antennas. The antennas are fed by a 2 GHz RF source with a 90° phase delay between adjacent pairs. The circularly polarized field drives the atoms into the m=28 circular state through the stepwise absorption of 28 photons. A detector in the circular state production region monitors the efficiency of the optical excitation and angular momentum transfer processes.

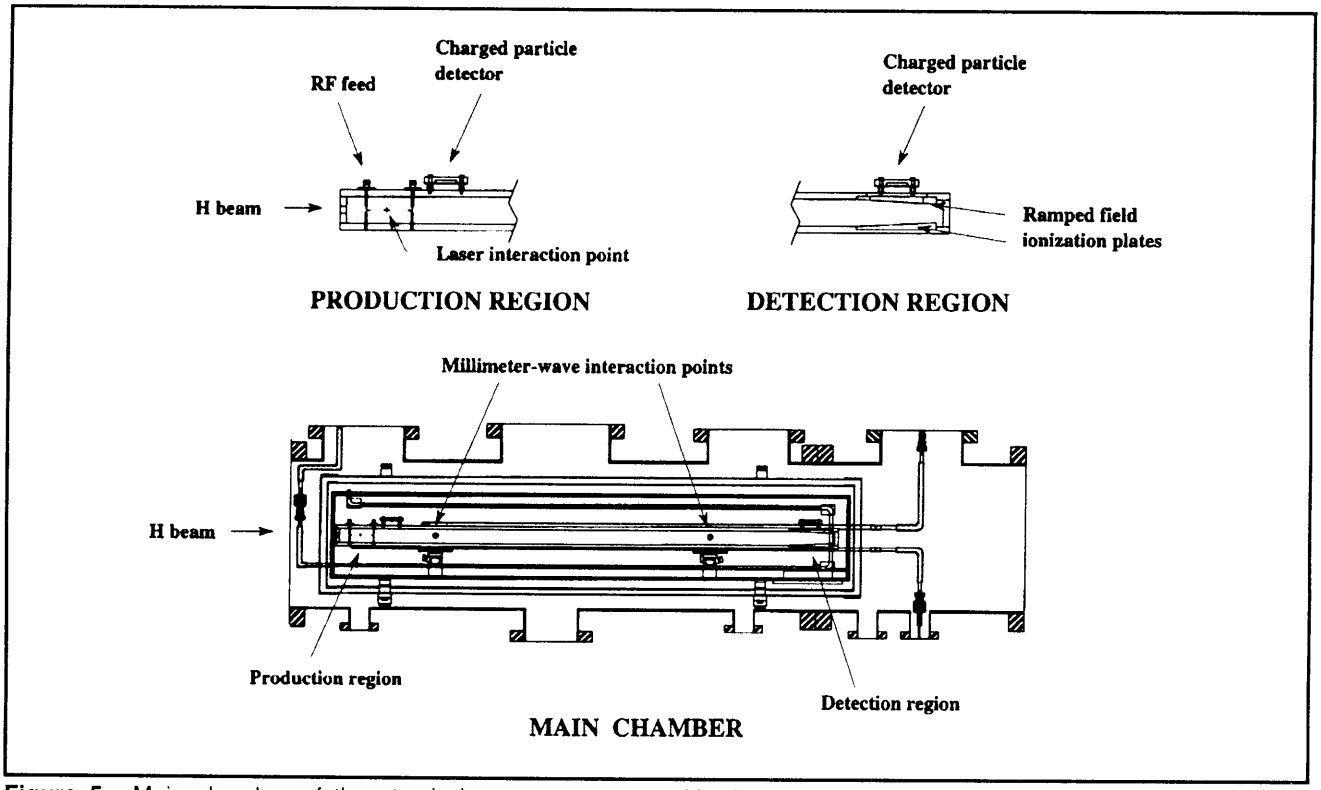

Figure 5. Main chamber of the atomic beam apparatus, with close-ups of the production region and the detection region.

After the atoms are prepared in the n=29 circular state, the beam enters the millimeter-wave interaction region. Because Rydberg atoms interact strongly with external fields, accurate measurement of the energy level structure requires careful control of the interaction environment. Thermal radiation is reduced by cooling the interaction region to ~ 10 K with a liquid helium flow system. The ambient magnetic field is reduced by a double-wall high-permeability shield. A small electric field, which defines the quantization axis of the atoms, is applied with high uniformity by field plates above and below the atomic beam. The millimeter-waves intersect the atomic beam at two locations separated by 50 cm. The millimeter-wave optical

[8] R. Hulet and D. Kleppner, "Rydberg Atoms in 'Circular' States," *Phys. Rev. Lett.* 51(16): 1430-1433 (1983).

system was described in a previous *Progress Report.*

The state distribution of the atoms emerging from the interaction region is analyzed by a state-selective electric field ionization detector. Within the detector, the atoms enter a region of increasing electric field produced by a symmetric pair of ramped plates held at constant potential. Atoms in different states ionized at different fields, and the charged nuclei are detected at different positions. The signals from individual atoms are time resolved. Because the source is pulsed, this allows contributions to the resonance pattern from each velocity class to be analyzed individually, providing a valuable measure of possible systematic errors.

Preliminary Ramsey interference data was presented in a previous *Progress Report.* The signal-to-noise ratio was too low to achieve the desired accuracy, but having demonstrated the feasibility of the method, we set about building a second-generation version of the apparatus designed to improve the signal-to-noise ratio by several orders of magnitude. We are nearing the end of this construction phase of the experiment.

The past year has been devoted to three major efforts: perfecting a new method of populating the initial circular state, building a new atomic beam interaction region and cooling system, and building a new high duty-cycle laser system.

Our original method of producing circular states used a magnetic field, which required that the production region be outside the magnetically shielded interaction region. We believe that this geometry introduced radiation leaks that significantly reduced our signal-to-noise ratio. The new circularization method described above does not require a magnetic field, and the production region is now located inside the magnetic shields.

Early during the past year, we finished testing the new technique, using a mock-up of the new production region. Field ionization signals indicate efficient transfer to the circular state (see figure 6). In the course of diagnosing the circular state production efficiency, we have found that our electric field ionization data agrees with exact numerical calculations. However, it differs significantly from a previously accepted semi-empirical formula which was found to be in good agreement with experiments using alkali metal atoms.[9] We are currently preparing a paper on the production of circular states in hydrogen.

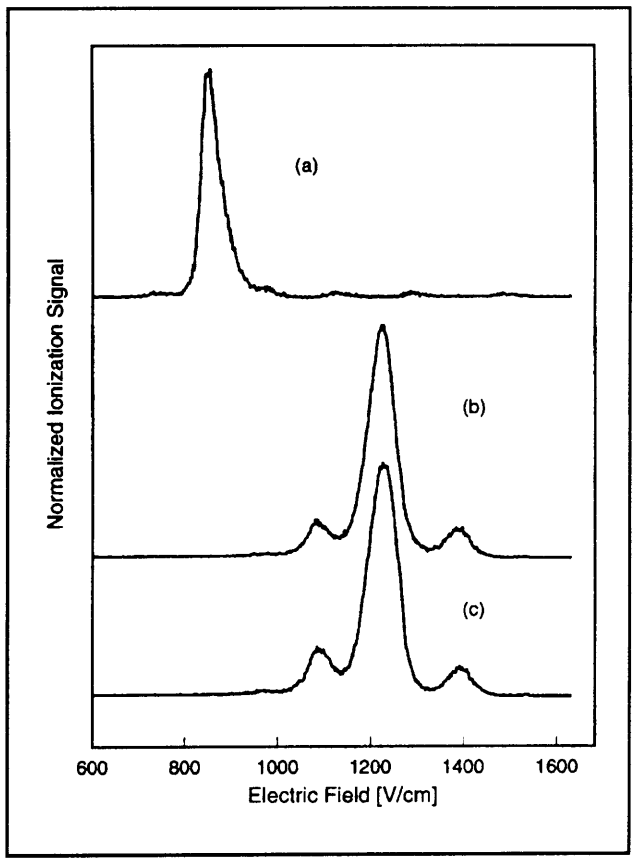

Figure 6. Production of "circular" states by absorption of circularly polarized 2 GHz radio-frequency radiation. The initial state, which ionizes at relatively low electric field (850 V/cm), is shown in (a). The two circular states are shown in (b) and (c). The characteristic ionization signal of the circular state appears at roughly 1220 V/cm.

By incorporating the production region into the magnetically shielded interaction region, it has been possible to consolidate the production, interaction, and detection regions into a monolithic helium temperature enclosure. We have completed much of this structure, including new field plates, liquid nitrogen temperature radiation shield, magnetic shields, and a precision supporting frame. We have also assembled a new helium flow system that should greatly reduce our liquid helium consumption rate, allowing longer data collection runs.

Finally, we are constructing a new ultraviolet dye laser system. Our original system was pumped with a YAG laser operating at 10 Hz. Since the transit time of even our slowest atoms is a few milliseconds, the duty cycle of the experiment was unnecessarily low. The new laser system, built

9 R.J. Damburg and V.V. Kolosov, "A Hydrogen Atom in a Uniform Electric Field III," *J. Phys. B.* 12(16): 2637-2643 (1979).

around an excimer pump laser, will run at 120 Hz. We are building our own tunable single-mode UV dye lasers to replace the yellow dye lasers used in the previous scheme. A pulsed wavemeter will allow calibration of the laser frequencies, which is an important advantage in setting up since there are no convenient atomic or molecular references at the wavelength of the UV dye lasers. With the completion of the laser system, we expect to begin taking data soon.

2.3 Precision Mass Spectrometry of Ions

Sponsors

Joint Services Electronics Program
Contract DAAL03-92-C-0001
Grant DAAH04-95-1-0038
National Science Foundation
Grant PHY 92-22768

Project Staff

Michael P. Bradley, Dr. Frank DiFilippo, Dr. Fred L. Palmer, Szymon M. Rusinkiewicz, Professor David E. Pritchard

In 1994, we published a table of ten atomic masses important for metrology or the determination of fundamental constants.[10] The accuracy of the masses in the table, typically 10^{-10}, represents one to three orders of magnitude improvement over previously accepted values. In addition, a wide variety of self-consistency checks allowed us to virtually eliminate the possibility of unknown systematic errors. This capability has allowed us to contribute to several important experiments in both fundamental and applied physics, including:

- Recalibration of the current x-ray wavelength standard by weighing the energy differences associated with the neutron capture gamma rays of ^{14}N, which are widely used as calibration lines.
- Determination of the atomic weight of ^{28}Si, part of a program to replace the "artifact" kilogram mass standard by a crystal of pure silicon, in effect creating an atomic standard of mass.
- Determination of the molar Planck constant $N_A\hbar$, by weighing γ-rays whose wavelength is to be accurately determined by a NIST group; this will also provide an independent determination of the fine structure constant.

In the fall of 1994, we made several important improvements to the stability and versatility of our mass spectrometer culminating in the demonstration of a technique for dramatically improving the accuracy of our mass comparisons by comparing two simultaneously trapped ions (to eliminate the problems due to field drift). In addition, we have demonstrated a squeezing technique to reduce the influence of thermal noise on the measurements. These advances led to another dramatic improvement in mass resolution that would allow:

- Determination of excitation and binding energies of atomic and molecular ions by weighing the small decrease in energy, $\Delta m = E_{bind}/c^2$. (We must reach our ultimate goal of a few x 10^{-12} to make this a generally useful technique.);
- Measurement of the ^3H-^3He mass difference, important in ongoing experiments to determine the electron neutrino rest mass;
- Improvement of some traditional applications of mass spectrometry resulting from our orders of magnitude improvement in both accuracy and sensitivity; and
- Determination of the molar Planck constant $N_A\hbar$, by measuring the atomic mass and recoil velocity of an atom that has absorbed photons of known wavelength.

Our experimental approach is to measure ion cyclotron resonance on a single molecular or atomic ion in a Penning trap, a highly uniform magnetic field in which confinement along the magnetic field lines is provided by much weaker electric fields. We monitor the ion's axial oscillation by detecting the currents induced in the trap electrodes using ultrasensitive superconducting electronics developed for this application.[11] This work in trapping and precision resonance draws on techniques developed by Hans Dehmelt at the University of Washington and Norman Ramsey at Harvard University, for which they shared the 1989 Nobel Prize.

We have developed techniques for driving, cooling, and measuring the frequencies of all three normal modes of ion motion in a Penning trap. Thus we can manipulate the ion position reproducibly to

---

[10] F. DiFilippo, V. Natarajan, K. Boyce, and D. E. Pritchard, *Phys. Rev. Lett.* 73: 1481 (1994).

[11] R. Weisskoff, G. Lafyatis, K. Boyce, E. Cornell, R. Flanagan, Jr., and D.E. Pritchard, *J. Appl. Phys.* 63: 4599 (1988).

within 30 microns of the center of the trap, correcting for electrostatic shifts in the cyclotron frequency to great accuracy. We use a π-pulse method to coherently swap the phase and action of the cyclotron and axial modes.[12] Therefore, although we detect only the axial motion directly, we can determine cyclotron frequency by measuring the phase accumulated in the cyclotron motion in a known time interval. We have implemented a new signal processing algorithm to improve our phase estimation by a factor of 2-3. We can measure the phase of the cyclotron motion to within 10 degrees, leading to a precision of 10^{-10} for a one minute measurement. Our entire ion-making process is fully automated, and the computer can cycle from an empty trap to having a cooled single ion in about three minutes under optimal conditions.

Careful shimming of the electric and magnetic fields allows us to keep our systematic errors well below 5×10^{-11}, but unfortunately, the typical statistical fluctuation in our magnetic field between measurements is 2.4×10^{-10}. Thus, even with the ability to achieve ~ 20 alternate loadings of two different ions in one night, our overall accuracy is at best 8×10^{-11} (see figure 7). We have found that the distribution of field variation is not Gaussian, but rather has too many outlying points. This has led us to use robust statistical analysis of field fluctuations; in particular a generalization of least squares fitting called "M-estimates" in which outlying points are deweighted in a manner determined by the observed excess number of outliers. This has eliminated arbitrary decisions about dropping "bad points" from our data sets and has increased the stability of our fits.

We have performed a wide variety of stringent checks for systematic errors. In fact, every mass in the table has been obtained from at least two independent sets of mass ratios. Several of the checks employ our new technique for comparison of non-doublets, pairs of ions whose nominal mass to charge ratios are unequal. This technique represents a significant advance in precision mass spectrometry since it allows us to obtain absolute masses by direct comparison to carbon, which is defined to have an atomic mass of exactly 12. It also provides an absolute check of our accuracy by allowing measurements that should verify known ratios such as N_2 and Ar^+/Ar^{++}. We have compared CD_4 and CD_3 to C to obtain two independent determinations of the atomic weight of deuterium. The results are consistent with the values for the

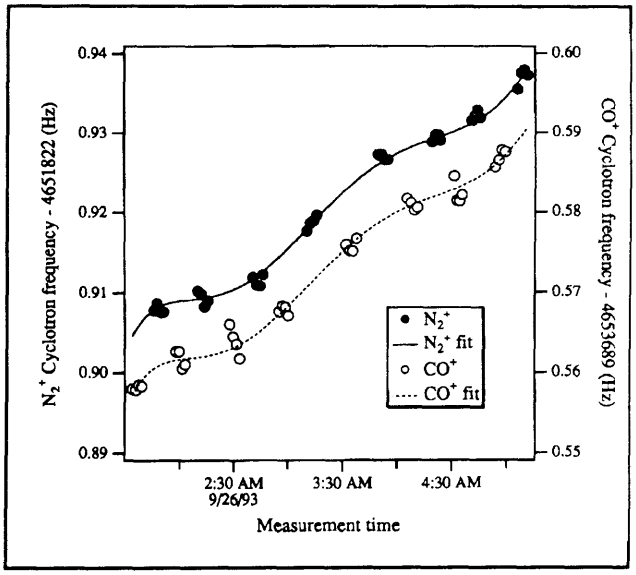

Figure 7. Cyclotron frequency as a function of time for alternate N_2^+ and CO^+ ions in our Penning trap. The frequencies are obtained after a 50s integration of cyclotron phase (see text). The solid line is a polynomial fit to the drift in the field common to both ions.

hydrogen masses we obtained from conventional doublet measurements. These carefully determined hydrogen and deuterium masses determine the mass of any organic compound composed of C, D, and H. The organic ions can in turn be used in doublet comparisons with many different ions. We have used this approach to obtain the absolute masses of several light atoms—H, D, N, O, Ne, Ar—to at least an order of magnitude better than the current standard mass table (see table 1).

An extensive series of quantitative systematic checks of our results using only doublet ratios was also performed. These include repeated checks of identical ratios (some interspaced by a significant reduction of our field inhomogeneities), checks of circular ratios (e.g., A/B, B/C, and C/A), and checks of related ratios (e.g., CO/N_2 and CO_2/N_2O). The consistency of all these checks practically guarantees that our errors are within the quoted limits.

Our newly rebuilt apparatus features improved stability of the trapping fields, a new and more efficient system for the ejection of unwanted ions, and most importantly, provisions for the excitation and detection of two different ions trapped at the same time. These improvements form the basis for an order of magnitude improvement in accuracy which will be achieved by simultaneous measurements on two ions to eliminate the problem of field fluctu-

[12] E.A. Cornell, R.M. Weisskoff, K. Boyce, and D.E. Pritchard, *Phys. Rev. A* 41: 312 (1992).

ations, and by using squeezing techniques to reduce thermal noise. We have expanded our previous theoretical understanding[13] of two ion dynamics to include the effects of minute imperfections in the trapping fields, and demonstrated the capability of this technique to reduce the effects of field fluctuations (figure 8). If this works as planned, the primary source of measurement noise will be the special relativistic mass shift due to thermal fluctuations in cyclotron amplitude. We have proposed several methods of classical squeezing with parametric drives to reduce amplitude fluctuations,[14] and demonstrated the simplest of these,[15] reducing thermal noise by about a factor of two. We have also built an external ion source and associated optics with which we plan to produce and select ions and guide them into the trap, thereby extending the types of ions we can measure.

Table 1. Atomic mass table. The center column lists the atomic masses determined from our experiment, and the right column lists the accepted atomic masses from the 1983 evaluation. For the purpose of comparision, zeros have been added to the numbers in the right column so that the number of digits are equal.

Atom	Mass (amu)	Accepted values (amu)
^{1}H	1.007 825 031 6 (5)	1.007 825 035 0 (120)
n	1.008 664 923 5 (23)	1.008 664 919 0 (140)
^{2}H	2.014 101 777 9 (5)	2.014 101 779 0 (240)
^{13}C	13.003 354 838 1 (10)	13.003 354 826 0 (170)
^{14}N	14.003 074 004 0 (12)	14.003 074 002 0 (260)
^{15}N	15.000 108 897 7 (11)	15.000 108 970 0 (400)
^{16}O	15.994 914 619 5 (21)	15.994 914 630 0 (500)
^{20}Ne	19.992 440 175 4 (23)	19.992 435 600 0 (22000)
^{28}Si	27.976 926 532 4 (20)	27.976 927 100 0 (7000)
^{40}Ar	39.962 383 122 0 (33)	39.962 383 700 0 (14000)

2.3.1 Publications

DiFilippo, F., V. Natarajan, K. Boyce, and D.E. Pritchard. "Accurate Masses for Fundamental Metrology." *Phys. Rev. Lett.* 73: 1481 (1994).

DiFilippo, F., V. Natarajan, M. Bradley, F. Palmer, and D.E. Pritchard. "Accurate Atomic Mass Measurements from Penning Trap Mass Comparisons of Individual Ions." *Physica Scripta.* Forthcoming.

DiFilippo, F., V. Natarajan, M. Bradley, F. Palmer, and D.E. Pritchard. "Accurate Atomic Mass Measurements from Penning Trap Mass Comparisons of Individual Ions," *Proceedings of the Fourteenth International Conference on Atomic Physics,* Boulder, Colorado, July 31-August 5, 1994. Forthcoming.

Natarajan, V., F. DiFilippo, and D.E. Pritchard. "Squeezed States of Classical Motion in a Penning Trap." Submitted to *Phys. Rev. Lett.*

---

[13] E.A. Cornell, K. Boyce, D.L.K. Fygenson, and D.E. Pritchard, *Phys. Rev. A* 45: 3049 (1992).

[14] F. DiFilippo, V. Natarajan, K. Boyce, and D.E. Pritchard, *Phys. Rev. Lett.* 68: 2859 (1992).

[15] V. Natarajan, F. DiFilippo, and D.E. Pritchard, "Classical Squeezing of a Oscillator for Sub-thermal Noise Operation," *Phys. Rev. Lett.* 74(15): 2855 (1995).

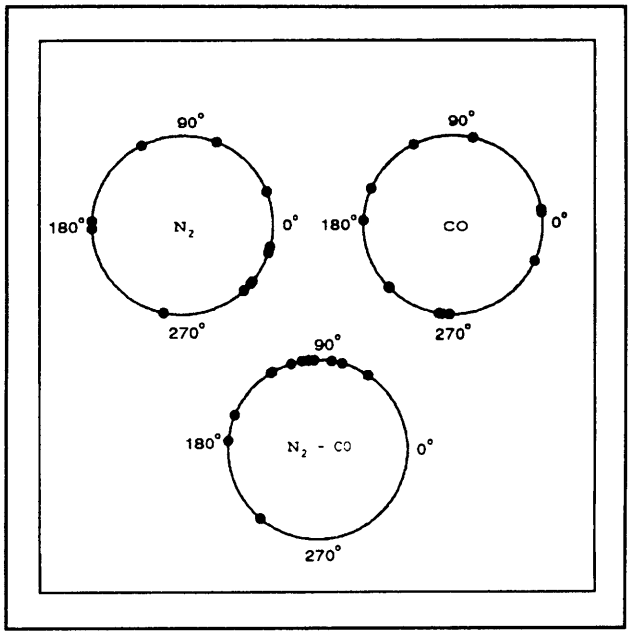

Figure 8. Each dot represents one measured cyclotron phase of simultaneously trapped single N_2^+ and CO^+ ions 16 seconds after excitation. Daytime field fluctuations have virtually randomized the phases of the individual ions but the phase difference between the two remains well defined.

2.3.2 Thesis

DiFilippo, F. *Precise Atomic Masses for Determining Fundamental Constants.* Ph.D diss., Dept. of Physics, MIT, 1994.

2.4 Atom Interferometry

Sponsors

Joint Services Electronics Program
Contract DAAL03-92-C-0001
Grant DAAH04-95-1-0038
U.S. Army - Office of Scientific Research
Grant DAAL03-92-G-0229
Grant DAAL01-92-6-0197
U.S. Navy - Office of Naval Research
Grant N00014-89-J-1207

Project Staff

Michael S. Chapman, Troy D. Hammond,[16] Dr. Alan L. Lenef, Amrit R. Pant, Richard A. Rubenstein, Dr. H. Jörg Schmiedmayer,[17] Edward T. Smith,[16] Bridget E. Tannian, Professor David E. Pritchard

The recent development of atom interferometers, in which atom or molecule de Broglie waves are coherently split, physically separated, and subsequently recombined to produce fringes represents a revolution in atomic physics. Atom interferometers give us the ability to measure accurately interactions that displace the phase or energy of the particles in one arm of the interferometer. This in turn allows us to make new qualitative measurements in atomic and molecular physics, fundamental tests of quantum mechanics, especially in areas involving atom-light interactions, and to measure acceleration and rotation in new ways.

- Atom interferometers permit completely new precision measurements of ground state properties of atoms and molecules. Important applications include precision measurements of atomic polarizabilities to test atomic structure models, measuring both molecular polarizability tensor components, and determining long range forces that are important in cold collisions and Bose-Einstein condensation.
- Atom interferometers have important applications to fundamental measurements in quantum mechanics. These include measurements of topological and geometric phases, loss of coherence to a reservoir, quantum measurement, and investigations of multi-particle interferometry and entanglement.
- The large mass and low velocities of atoms makes atom interferometers especially sensitive to inertial effects like acceleration and rotation. They have a potential sensitivity to rotations that is $\sim 10^{10}$ greater than an optical interferometer of the same area.
- Atom interferometers may have significant application to condensed matter physics, including measurement of atom-surface interactions and lithography using coherently manipulated fringe patterns that are directly deposited onto substrates.

Our group has been a pioneer in the area of atom optics and atom interferometry, demonstrating the first nanofabricated diffraction gratings for atoms and using them to study atomic Talbot re-imaging of grating patterns, an effect that may have impor-

---

[16] Partially supported by a National Science Foundation Fellowship.

[17] Partial support from the Universitaet Innsbruck; partial support from an APART Fellowship of the Austrian Academy of Sciences.

tant lithographic applications.[18] We used these gratings to make the first atom interferometer in which the atom waves traverse physically separated paths. We have pioneered the scientific applications of atom interferometers by using this instrument to make accurate measurements of atomic polarizability,[19] and the first measurements of the index of refraction of gas for incident matter waves traversing a gas.[20] We have made a molecular interferometer, demonstrating that complex particles with a large number of populated internal states can exhibit high contrast interference.[21]

During 1994, we performed atom interferometer experiments to test fundamental concepts of coherence in quantum interference and began an experiment to investigate the very high intrinsic sensitivity of atom interferometers to acceleration and rotation. In 1995, we have also completed and submitted several major papers, some of which are already in press. These include papers on atomic polarizability, index of refraction of matter waves, near field imaging (atomic Talbot effect), molecule optics and interferometry, and a proposed new velocity selection scheme for precision measurements.

The key element in our interferometer (figure 9) is the set of three matched transmission diffraction gratings with a 200 nm period that we fabricated at the National Nanofabrication Facility (NNF) at Cornell University using a process that we developed there. One of the important contributions this year has been the development of an alignment process to eliminate edge discontinuities or "stitches" between the adjacent 50 μm^2 fields when writing large patterns. This has produced our most coherent gratings to date, resulting in a measured fringe contrast of nearly 45 percent. We also produced new 140 and 160 nm period grating sets, together with new non-magnetic silicon nitride collimating slits.

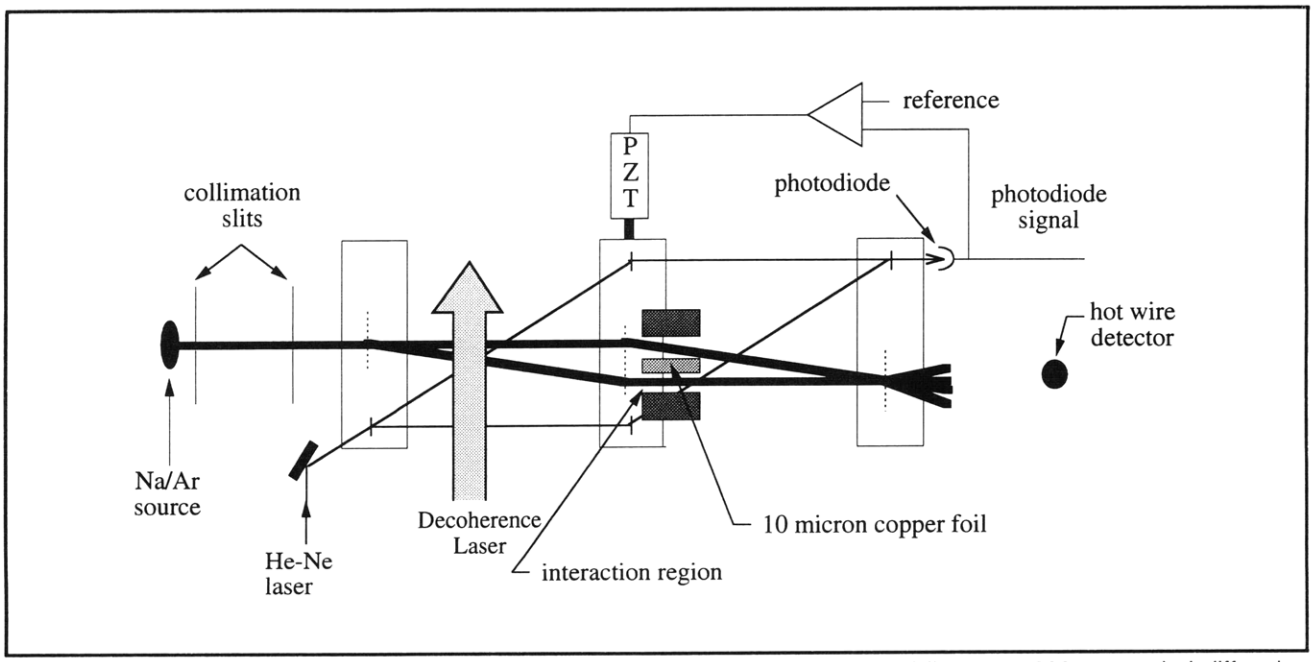

Figure 9. Schematic of our interferometer and interaction region. Vertical dashed lines are 200 nm period diffraction gratings. The interaction region used in measurements of fundamental phases and atomic and molecular properties is inserted between the atom waves. A focused laser applies π-pulses to scatter photons in decoherence and recoherence experiments. Scattering of photons produces a phase shift in each de Broglie wave path that depends upon separation of de Broglie waves.

---

[18] M.S. Chapman et al., "Near Field Imaging of Atom Diffraction Gratings: the Atomic Talbot Effect," *Phys. Rev. A* 51: R14 (1994).

[19] C.R. Ekstrom, J. Schmiedmayer, M.S. Chapman, T.D. Hammond, and D.E. Pritchard, "Measurement of the Electric Polarizability of Sodium with an Atom Interferometer," submitted to *Phys. Rev. A.*

[20] J. Schmiedmayer, M.S. Chapman, C.R. Ekstrom, T.D. Hammond, S. Wehinger, and D.E. Pritchard, "Index of Refraction of Various Gases for Sodium Matter Waves," *Phys. Rev. Lett.* 74: 1043 (1995).

[21] M.S. Chapman et al., "Optics and Interferometry with Molecules," *Phys. Rev. Lett.,* forthcoming.

2.4.1 Quantum Interference and Coherence

We integrated a dye laser into our apparatus to investigate photon-atom interactions in the interferometer and to polarize the atom beam by optical pumping techniques. This permitted us to investigate the loss of coherence or "decoherence" between the two separated de Broglie wave components when resonant single photons are scattered in the interferometer (figure 9). The fringe contrast and phase shift are measured as a function of separation between the two paths. We found that fringe contrast decreases significantly when the separation exceeds about $\lambda_{photon}/4$, in accordance with the expectations of Bohr's complimentarity principle. However, contrast at larger separations also exhibits strong revivals (figure 10), as predicted by our theory.[22]

In recent theoretical and experimental investigations of spontaneous emission from interfering atom de Broglie waves,[23] coherence loss can be naturally interpreted as a smearing or "diffusion" of the atom fringes by the random photon recoil kicks. One of the important implications of our experiment is that contrast loss in our interferometer clearly arises from an averaging over phase differences imparted to the two interfering de Broglie waves by the scattering photon, rather than displacements of the scattered atom by the photon recoil.

We modified our decoherence experiment to take advantage of the correlation or entanglement between scattered photons and the phase difference imparted to the de Broglie waves. By using highly collimated beams and a narrow slit in front of the detector, we could select only atoms that scattered photons within a limited range of photon recoil momenta. For these atoms, we find that the fringe contrast persists over significantly larger path separations than in our "decoherence" experiment (figure 10). We call this a "recoherence" experiment. It explicitly shows, for the first time, that resonantly scattering a photon from an atom does not irreversibly destroy the atomic coherence.

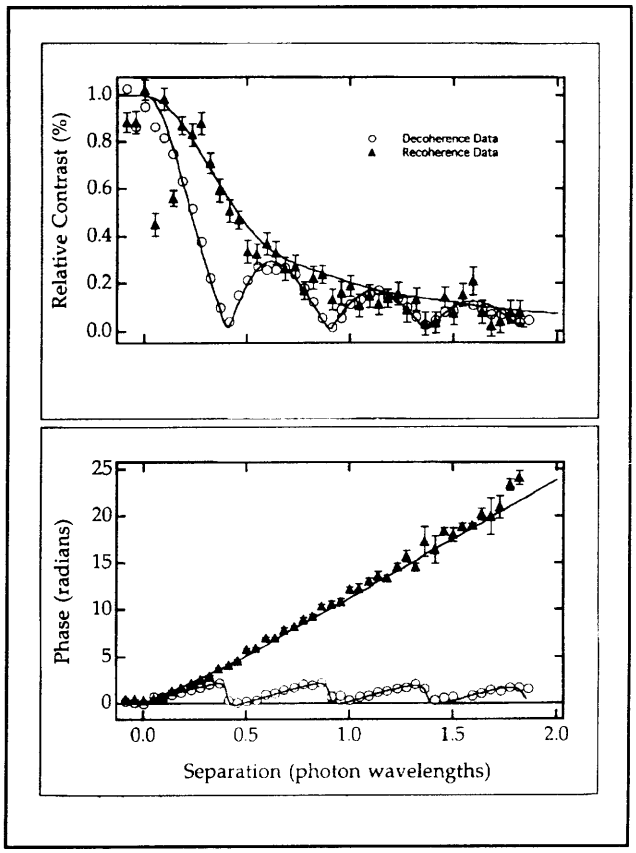

Figure 10. Results of light scattering experiment. (upper plot) Contrast versus separation between de Broglie wave components in optical wavelengths. Decoherence data (circles) shows fringe contrast decreasing rapidly but with revivals. Recoherence data (triangles shows a more gradual decrease in fringe contrast from sub-photon recoil momentum resolved detection of atoms. (lower plot) Phase versus separation between de Broglie wave components in optical wavelengths for decoherence data (circles) and recoherence data (triangles).

2.4.2 Inertial Effects

Phase shifts that arise from the path length differences in interfering de Broglie waves in accelerating frames have been discussed by many authors in both non-relativistic and relativistic contexts.[24] Recently, we have obtained preliminary results in which we measured rotations of our interferometer at rotation speeds of about one earth rate (7.3×10^{-5} rads/ sec) (figure 11). This is about three-orders of magnitude more sensitive than pre-

---

[22] M.S. Chapman et al., "Loss of Coherence by a Single Scattering Event," to be submitted.

[23] T. Pfau, S. Spälter, C. Kurstsiefer, C.R. Ekstrom, and J. Mlynek, "Loss of Spatial Coherence by a Single Spontaneous Emission," *Phys. Rev. Lett.* 29: 1223 (1994); D.F. Walls in "Laser Manipulation of Atoms and Ions," Varenna, 1991, E. Arimondo, E.D. Phillips and F. Strumia, (North Holland: Amsterdam, 1992).

[24] J. Anandan, *Phys. Rev. Lett.* 48: 1660 (1982).

vious measurements of rotation using atom interferometry and shows the promise of using atom interferometers for inertial navigation systems. We expect to be able to measure rotations to less than 5×10^{-4} earth rates with one hour of integration time and demonstrate accuracies below one percent at higher rotation rates. This is close to the performance of the best commercial laser gyroscopes. Improvements in our current nanofabrication technology to make 1 cm^2 gratings coupled with slower, high flux, effusive cesium beams should lead to much greater detectivities ($\sim 10^{-7}$-10^{-8} earth rates for one hour integration).

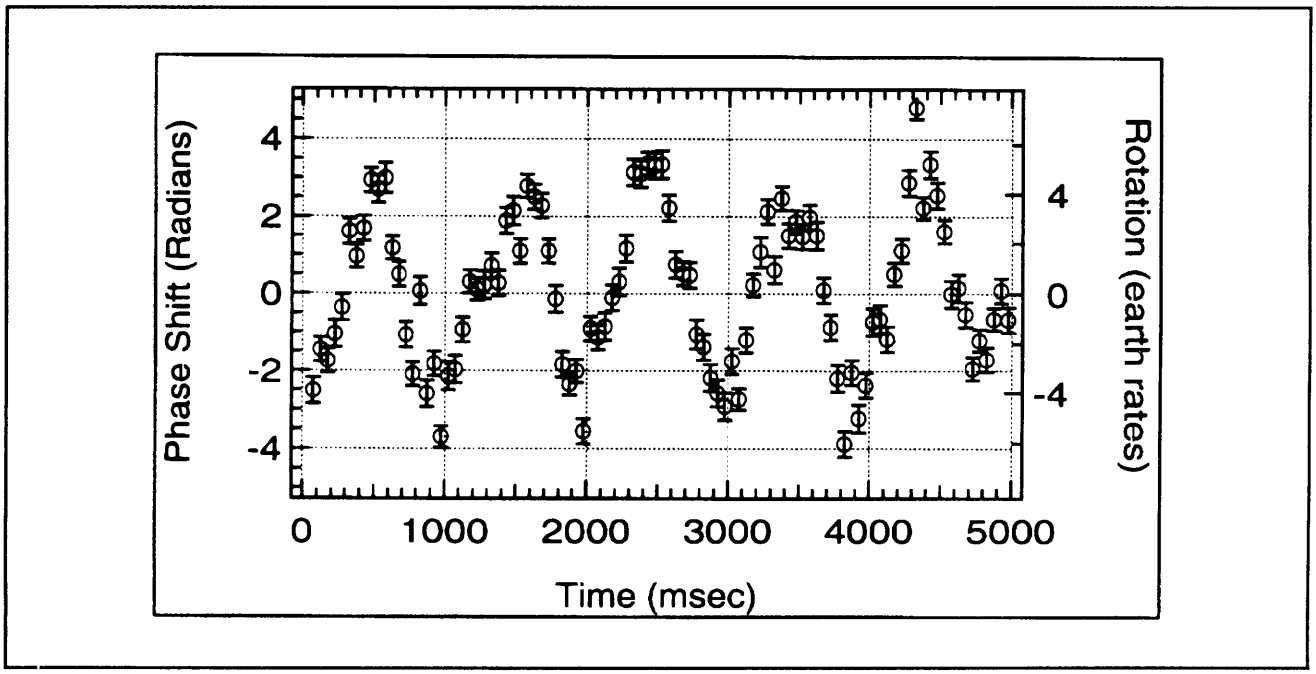

Figure 11. Experimental data showing measured phase versus time for a sinusoidal rotating excitation at approximately 1 Hz. The corresponding estimated rotation rates are shown in units of earth rates (7.3×10^{-5} rad/sec).

2.4.3 New Precision Measurements

In order to improve the precision of atom and molecular interferometry measurements, we have proposed a promising high-flux velocity selection technique that will permit the application of large phase shifts without loss of fringe contrast due to the velocity dependence of the phase for most applied potentials. In this approach, which we call "velocity multiplexing," a potential is applied such that the phase shifts of atoms in the peaks of a multi-peaked velocity distribution are exact integral multiples of 2π. Thus, interference patterns from each of the velocity peaks add constructively to produce high fringe contrast at very large applied phase shifts. This technique appears capable of measurements with less than 0.1 percent errors.

In future experiments, we plan to perform precision measurements of the Aharonov-Casher (AC) phase and Berry's phase using our separated beam interferometer. We will be able to achieve up to 1 radian AC phase shift in our interferometer, significantly greater than in previous experiments that use much weaker neutron spins. This will allow us to study the predicted dependence on the dipole orientation for the first time. With further modifications to our interaction region to introduce spatially varying magnetic fields, we will also investigate the geometric or Berry's phase.

2.4.4 Publications

Chapman, M.S., C.R. Ekstrom, T.D. Hammond, R. Rubenstein, J. Schmiedmayer, S. Wehinger, and D.E. Pritchard. "Optics and Interferometry with Molecules." Submitted to *Phys. Rev. Lett.*

Chapman, M.S., C.R. Ekstrom, T.D. Hammond, J. Schmiedmayer, B.E. Tannian, S. Wehinger, and D.E. Pritchard. "Near Field Imaging of Atom Diffraction Gratings: the Atomic Talbot Effect." *Phys. Rev. A* 51: R14 (1995).

Ekstrom, C.R., J. Schmiedmayer, M.S. Chapman, T.D. Hammond, and D.E. Pritchard. "Measurement of the Electric Polarizability of Sodium with an Atom Interferometer." Submitted to *Phys. Rev. A.*

Hammond, T.D., D.E. Pritchard, M.S. Chapman, A. Lenef, and J. Schmiedmayer. "Multiplex Velocity Selection for Precision Matter Wave Interferometry." *App. Phys. B.* Forthcoming.

Pritchard, D.E. "Atom Interferometer." *Proceedings of the 13th International Conference on Atomic Physics.* Eds. T.W. Hansch, H. Walther, and B. Neizert. New York: American Institute of Physics, 1993.

Pritchard, D.E., M.S. Chapman, C.R. Ekstrom, T.D. Hammond, J. Schmiedmayer, A. Lenef, R. Rubenstein, and S. Wehinger. "Interferometry with Atoms and Molecules." In *Fundamental Problems in Quantum Theory.* Proceedings of the New York Academy of Sciences, Baltimore, Maryland, June 18-22, 1994. Forthcoming.

Pritchard, D.E., C.R. Ekstrom, J. Schmiedmayer, M.S. Chapman, and T.D. Hammond. "Atom Interferometry." *Proceedings of the Eleventh International Conference on Laser Spectroscopy,* June 13-18, 1993. Eds. L.A. Bloomfield, T.F. Gallagher, and D.J. Larson. New York: American Institute of Physics, 1993.

Pritchard, D.E., T.D. Hammond, J. Schmiedmayer, C.R. Ekstrom, and M.S. Chapman. *Proceedings of the Conference on Quantum Interferometry,* Trieste, Italy, March 2-5, 1993. Eds. F. DeMartini, A. Zeilinger, and G. Denardo. Singapore: World Scientific, 1993.

Schmiedmayer, J., M.S. Chapman, C.R. Ekstrom, T.D. Hammond, S. Wehinger, and D.E. Pritchard. "Index of Refraction of Various Gases for Sodium Matter Waves" *Phys. Rev. Lett.* Forthcoming.

Schmiedmayer, J., C.R. Ekstrom, M.S. Chapman, T.D. Hammond, and D.E. Pritchard. "Atom Interferometry." *Proceedings of the Seminar on Fundamentals of Quantum Optics III,* Kuhtai, Austria, 1993. Ed. F. Ehlotzky. Berlin: Springer-Verlag, 1993.

Schmiedmayer, J., C.R. Ekstrom, M.S. Chapman, T.D. Hammond, S. Wehinger, and D.E. Pritchard. "Magnetic Coherences in Atom Interferometry." *J. Phys. II* (France) 4: 2029 (1994).

2.4.5 Thesis

Tannian, B. *Near Field Imaging of Atomic Diffraction Gratings: The Atomic Talbot Effect.* B.S. thesis. Dept. of Physics, MIT, 1994.

2.5 Cooling and Trapping Neutral Atoms

Sponsors

Alfred P. Sloan Foundation
Joint Services Electronics Program
Contract DAAL03-92-C-0001
Grant DAAH04-95-1-0038
U.S. Navy - Office of Naval Research
Grant N00014-90-J-1642
Grant N00014-94-1-0807

Project Staff

Professor Wolfgang Ketterle, Michael R. Andrews, Kendall B. Davis, Marc-O. Mewes, Ilya Entin, Philip M. Hinz, Everest W. Huang, Wan Y. Morshidi, Stanley H. Thompson, John J. Wuu, Peter S. Yesley

2.5.1 Introduction and Summary

Cooling and trapping of neutral atoms offers exciting new possibilities. Many are related to the fact that the deBroglie wavelength increases with decreasing temperature T as $1/\sqrt{T}$. When the deBroglie wavelength is comparable to atomic dimensions (range of the interaction potential) collisions can no longer be treated classically. They are dominated by weak long-range interactions. Since the collision duration for slow atoms greatly exceeds the radiative decay time, stimulated and spontaneous radiative transitions can take place during the collision. Slow collisions are therefore fundamentally different from the fast collisions which have been studied so far, and they are becoming an exciting new field of atomic physics. Dramatic effects are expected for even colder temperatures and higher densities, when the deBroglie wavelength becomes comparable to the interatomic spacing. In this case, the "atomic waves overlap" and a novel type of highly correlated quantum matter is predicted, but has not yet been observed. In the case of bosonic atoms, one expects the formation of a Bose condensate, a macroscopic population of a single quantum state,[25] and phenomena

[25] K. Huang, *Statistical Mechanics,* 2nd ed. (Wiley: New York, 1987).

similar to superconductivity or superfluidity; fermions would form a highly correlated Fermi sea.

Such strongly correlated atoms are predicted to exhibit unusual behavior both in their interaction with light and in collisions. Furthermore, such samples of atoms have potential applications in the field of atom optics, such as in the creation of microscopic structures by direct-write lithography or in atom microscopy. Structures as small as 65 nm were obtained recently by laser-focused atomic deposition,[26] mainly limited by the transverse collimation and the thermal velocity spread of the atomic beam. Improvements by an order of magnitude should be possible. With coherent atoms, one could realize the ultimate resolution in focusing atoms which is analogous to the diffraction limit in optics. A Bose condensate would also find application in metrology, improving frequency standards and atom interferometry. Cesium clocks using microkelvin atoms might improve the accuracy of the current frequency standard by two orders of magnitude.[27] Nanokelvin atoms will offer additional improvements.

Despite the rapid progress in laser cooling over the last few years, the conditions necessary to observe degenerate quantum gasses have not yet been achieved. This is related to the fact that temperatures well below the recoil-limit are necessary (i.e., kinetic energies should be much less than the recoil energy due to the emission of a single photon). Although optical sub-recoil cooling is possible, it has severe limitations due to collisions of excited atoms and absorption of scattered light.

Our approach is to use evaporative cooling which does not involve light and therefore has no recoil limit to overcome. The cooling is accomplished by selectively removing atoms with the highest energy from the trap and then allowing the rest of the sample to rethermalize through elastic collisions. Unfortunately, this method requires high initial densities which, until recently, could only be prepared by cryogenic methods applicable solely to atomic hydrogen.[28] By using a combination of different cooling and trapping techniques involving lasers and magnetic fields, we can now obtain high initial density and observe evaporative cooling. This closes the gap between optical cooling at relatively low density and collisional cooling. It frees evaporative cooling from the restrictions of a cryogenic environment by using laser cooling as the precooling stage. In our initial experiments, the temperature was reduced by a factor of twelve and the phase space density increased by more than two orders of magnitude.[29] We are optimistic that experimental improvements will result in even colder temperatures in the near future. These results and other projects will now be described in greater detail.

2.5.2 Magnetic Trapping of Sodium Atoms

We have captured more than 10^{10} atoms in a dark light trap and transferred them into a magnetic trap. Initial atomic densities in the magnetic trap were 10^{11} atoms cm^{-3}. Much higher atomic densities have been obtained by subsequent adiabatic compression. A slow increase of the magnetic field gradient to 1000 G/cm resulted in ten times higher densities at five times higher temperatures. Although there is no gain in phase space density, adiabatic compression resulted in a substantial speedup of evaporative cooling due to an increase in the elastic collision rate by a factor of twenty. The thermalization time in the compressed cloud was only 50 ms, much shorter than the lifetime of the sample which was 30 seconds, due to the residual pressure of $5\ 10^{-11}$ mbar.

2.5.3 Elastic Cross Section of Ultracold Sodium Atoms

The driving process for evaporative cooling is elastic collisions. Although the interaction potential between two sodium atoms at long range is fairly well known (van der Waals potential), the low temperature elastic cross section cannot be accurately predicted. The reason is that only one partial wave (s-wave) contributes to the scattering of sodium atoms below 1 mK. Depending on the scattering phase shift, the zero-temperature cross section varies between zero and infinity. The phase shift depends critically on the binding energy of the last bound vibrational level and is very sensitive to fine details of the interaction potential.

---

[26] J.J. McClelland, R.E. Scholten, E.C. Palm, and R.C. Celotta, *Sci.* 262: 877 (1993).

[27] K. Gibble and S. Chu, *Metrologia* 29: 201 (1992).

[28] N. Masuhara et al., *Phys. Rev. Lett.* 61: 935 (1988).

[29] K.B. Davis, M.-O. Mewes, M.A. Joffe, M.R. Andrews, and W. Ketterle, submitted to *Phys. Rev. Lett.*

We were able to deduce the elastic collision cross section by observing the thermalization of an atom cloud. For this, a non-thermal distribution was prepared by temporarily displacing the trap center along the symmetry axis resulting in an elongated cloud. Using absorption imaging, the relaxation of this anisotropic energy distribution was observed by recording the shape of the cloud as a function of time.[30] In principle, equilibration might happen due to the ergodic evolution of orbits in the trap independent of collisions. However, this effect was ruled out by showing that the equilibration time depended linearly on density.

From the thermalization time, we derived the elastic cross section $\sigma = 6.0 \pm 3.0\ \mathrm{cm}^{-12}$. The measurement was performed at 200 μK, well below the temperature (1 mK) at which one expects d-wave contributions or a temperature dependence of the s-wave cross section. We can therefore deduce the scattering length $a = \pm (92 \pm 25)\ a_0$ using the relation $\sigma = 8\pi a^2$. Recently, accurate calculations of the scattering length of cold sodium atoms have been performed. For sodium atoms in the $F = 1$, $m_F = -1$ state result was $56\ a_0 < a < 154\ a_0$ and, for an alternative choice of potentials $-36\ a_0 < a < 154\ a_0$.[31] Thus, those calculations could not rule out negative values of the scattering length which would result in an unstable Bose condensate. Our experimental result, together with the theoretical prediction, show that sodium in the $F = 1$, $m_F = -1$ state has a large positive scattering length and is therefore an ideal choice for the pursuit of Bose Einstein condensation in alkali atoms.

2.5.4 Rf Induced Evaporative Cooling of Atoms

We want to reach the nK regime using evaporative cooling. Evaporative cooling is accomplished by repetitively removing the high energy "tail" of the thermal distribution of atoms in the trap.[32] The remaining atoms then cool collisionally as the high energy "tail" is repopulated. The essential condition for evaporative cooling is that the collision rate is sufficiently high for many collisions to occur within the lifetime of the atoms in the trap. In addition to high initial density and long trapping times, evaporative cooling requires a method for selectively removing hot atoms from the trap. In rf induced evaporation, atoms are spinflipped to an untrapped state when they are in resonance with an applied rf field.[33] Since this resonance frequency is a function of magnetic field B, atoms are selectively removed at a specific value of B. In the case of transitions between magnetic sublevels m_F, the resonance frequency is $\omega_{rf} = |g| \mu_B B/\hbar$, where g is the g-factor and μ_B the Bohr magneton. Since the trapping potential is given by $m_F g \mu_B B(r)$, only atoms which have a total energy $E > \hbar\omega_{rf} |m_F|$ will evaporate; or in other words, application of rf radiation of frequency ω_{rf} creates a trap "lip" with a height of $\hbar\omega_{rf} |m_F|$. An advantage is that the "lip" exists over a large surface rather than a small saddle point region of the trap.[34]

We observed temperature reduction by a factor of 12 and a simultaneous increase in density by a factor of 3.5 resulting in an increase in phase space density by a factor of 140. Evaporation was performed in such a way that the elastic collision rate, which is proportional to density times velocity, increased during evaporation. We are therefore already in the regime where evaporative cooling is self-accelerating. Indeed, one expects "run-away" evaporation when the number of collisions during a trapping time exceeds 25.[35] With an estimated collision rate of 50/s in the compressed cloud, we exceed this value by about a factor of 60. The cloud after evaporation had a temperature of 80 μK and a density of $2\ 10^{12}\ \mathrm{cm}^{-3}$. This phase space density is $2\ 10^4$ times smaller than required for Bose-Einstein condensation.

The current limitation of our evaporative cooling is an increased trap loss for small atom clouds. For the coldest temperatures achieved, the trapping time decreases from 30 s to a few seconds. This is probably due to Majorana flops, non-adiabatic transitions to an untrapped state which happen near

---

30 C.R. Monroe, E.A. Cornell, C.A. Sackett, C.J. Myatt, and C.E. Wieman, *Phys. Rev. Lett.* 70: 414 (1993).

31 A.J. Moerdijk and B.J. Verhaar, *Phys. Rev. Lett.* 73: 518 (1994).

32 H.F. Hess, *Phys. Rev. B* 34: 3476 (1986).

33 D.E. Pritchard, K. Helmerson, and A.G. Martin, "Proceedings of the 11th International Conference on Atomic Physics 11," in *Atomic Physics*, eds. S. Haroche, J.C. Gay, and G. Grynberg (Singapore: World Scientific, 1989) p. 179.

34 N. Masuhara et al., *Phys. Rev. Lett.* 61: 935 (1988).

35 K.B. Davis, M.-O. Mewes, and W. Ketterle, *Appl. Phys. B* 60: 155 (1995).

the center of the trap where the magnetic field vanishes.[36] Further progress should be possible after transferring the atoms into a trap with a different field geometry which does not have zero magnetic field in the center.

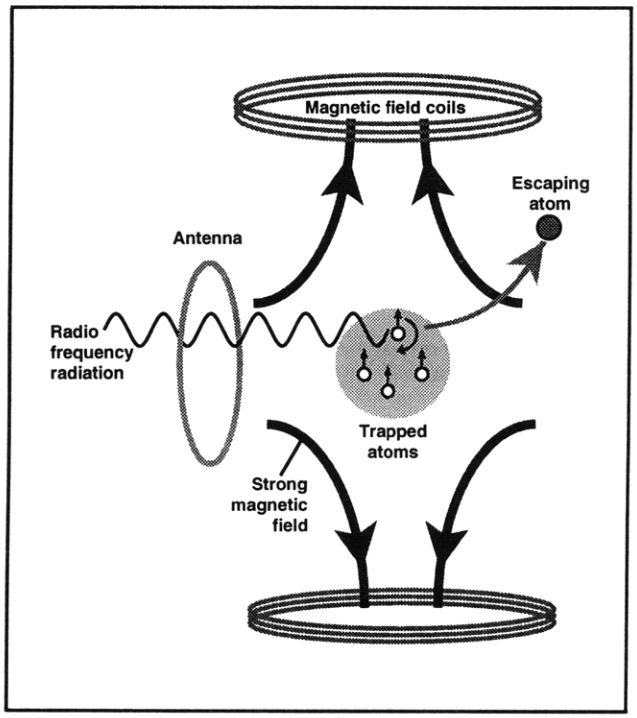

Figure 12. Experimental setup for forced evaporation. Neutral atoms are magnetically trapped. Radio-frequency radiation is tuned into resonance with the most energetic atoms in the thermal distribution. These atoms are spin-flipped to an untrapped state and ejected from the trap. The temperature of the remaining atoms is reduced by collisional thermalization.

2.5.5 An Analytical Model for Evaporative Cooling

In a recent theoretical paper, we describe an analytical model for evaporative cooling.[37] By simulating evaporation as a discrete process, we could predict the time dependence of all important parameters such as temperature, density, and elastic collision rate. By incorporating trap loss due to background gas collisions into our model, we predicted the threshold conditions for "run-away" evaporation. This is characterized by an increase in the thermalization rate during the cooling process. This model has proven to be valuable in understanding the experimental results.

2.5.6 Lithium Experiment

In addition to the sodium experiment, we are currently working on an intense source of cold lithium atoms. The long term goal is to observe quantum-statistical effects in a fermionic system (^{6}Li) in direct comparison with a bosonic system (^{7}Li). During the last year, two dye lasers were set up providing tunable single-mode light at 671 nm, the wavelength of the Li D-line. In order to lock the lasers to a Doppler free resonance, a lithium vapor cell and a phase modulator driven by a resonant transformer were built.

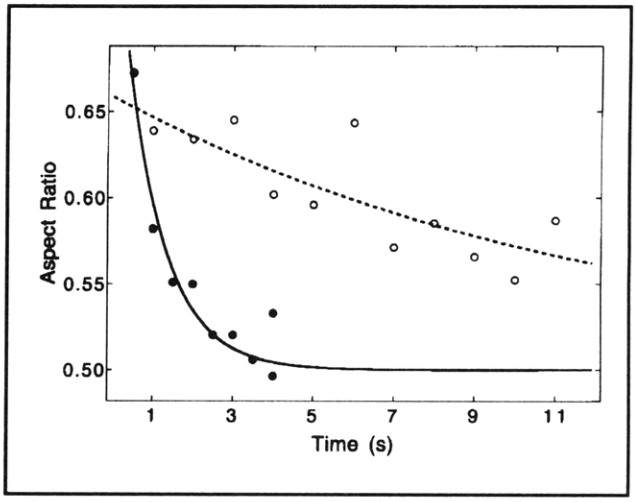

Figure 13. Thermal relaxation of an atom cloud after one-dimensional heating. The figure shows the aspect ratio of the cloud versus time for two different initial densities (solid circles: 5 10^{10} cm^{-3}, open circles: 4 10^9 cm^{-3}). The lines represent simple exponential fits with time constants of 1.0 s and 13 s, respectively.

[36] T.H. Bergeman, P. McNicholl, J. Kycia, H. Metcalf, and N.L. Balazs, *J. Opt. Soc. Am. B* 6: 2249 (1989).

[37] K.B. Davis, M.-O. Mewes, and W. Ketterle, *Appl. Phys. B* 60: 155 (1995).

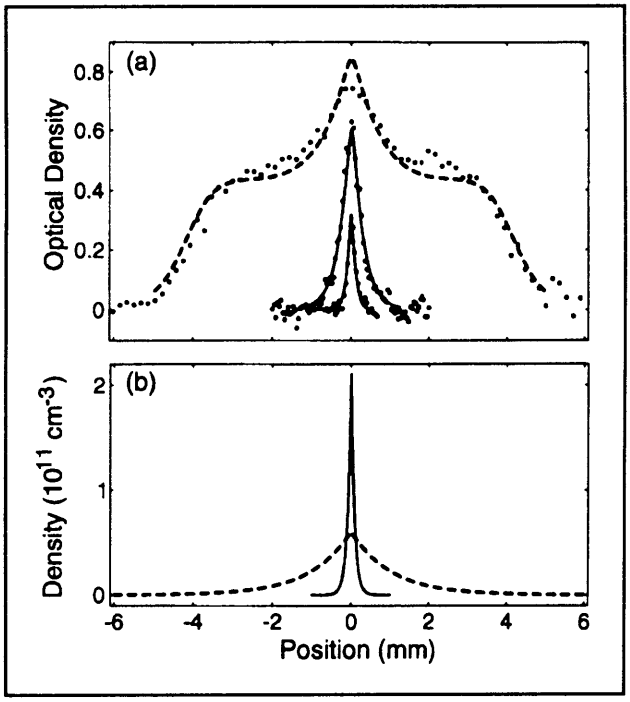

Figure 14. Optical density (a) and density (b) before and after evaporative cooling. The initial temperature was reduced by a factor of twelve. At the same time, the density increased, despite the loss in the number of trapped atoms.

2.5.7 Publications

Davis, K.B., M.-O. Mewes, M.A. Joffe, M.R. Andrews, and W. Ketterle. "Evaporative Cooling of Sodium Atoms." Submitted to *Phys. Rev. Lett.*

Davis, K.B., M.-O. Mewes, and W. Ketterle. "An Analytical Model for Evaporative Cooling of Atoms." *Appl. Phys. B* 60: 155 (1995).

2.5.8 Published Conference Papers

Davis, K.B., M-O. Mewes, M.A. Andrews, and W. Ketterle. "Transfer of Laser-cooled Atoms into a Magnetic Trap." OSA Annual Meeting, Dallas, Texas, 1994, Program p. 135, Abstract WPP3.

Davis, K.B., M-O. Mewes, M.A. Joffe, and W. Ketterle. "Evaporative Cooling of Sodium Atoms." 14th International Conference on Atomic Physics (ICAP), Boulder, Colorado, 1994, Book of Abstracts, Paper 1M-3.

Ketterle, W. "Cooling and Trapping of Neutral Atoms." The Future of Spectroscopy: From Astronomy to Biology, Quebec, Canada, September 1994, *National Research Council Canada, Book of Abstracts,* p. 34.

Ketterle, W., K.B. Davis, M.A. Joffe, M.-O. Mewes, and D.E. Pritchard. "Dark Cold Atoms at High Densities." International Quantum Electronics Conference (IQEC), Anaheim, California, 1994. *1994 Technical Digest Series,* Vol. 9. Washington, D.C.: Optical Society of America, 1994, p. 236.

Mewes, M.-O., K.B. Davis, P. Yesley, M.A. Joffe, D.E. Pritchard, and W. Ketterle. "A Spin-flip Zeeman Slower for the Production of Intense Slow Sodium Beams." *OSA Annual Meeting,* Dallas, Texas, 1994, Abstract WPP4, Program p. 135.

2.5.9 Thesis

Morshidi, W.Y. *Frequency Modulation Spectroscopy for Frequency Stabilization of Dye-laser.* B.S. thesis. Dept. of Phys., MIT, 1994.